Reduced order models in reactor kinetics: A comparison between point kinetics and multipoint kinetics

G. Valocchi, J. Tommasi, P. Ravetto

Version of Record: https://www.sciencedirect.com/science/article/pii/S030645492030400X
Manuscript_089032b137f8b62a2f0b24427138a141

Reduced order models in reactor kinetics: a comparison between point kinetics and multipoint kinetics

G. Valocchi, J. Tommasi and P. Ravetto

Abstract

Due to the heavy computational burden of full reactor kinetics modeling, reduced-order models are usually employed to simulate transients. Among those, point and multipoint kinetics have small computation time and provide satisfying results for many applications. We implemented point and multipoint kinetics (Avery's and Kobayashi's models) in the APOLLO3 code. Then these models are applied to study two simple transients, one in a coupled fast-thermal configuration, the other in a fast reactor. As at present we focus on the neutronic response only (neutron and precursor populations), the study is limited to step-change transients with no thermal feedback. This work permits to better delineate the potential of these methods and opens interesting perspectives. As an example, multipoint kinetics allows accounting for very fast shape transients that, depending on the coupling of the system, may result in global population changes occurring before the conventional prompt jump and altering significantly its quantitative value.

Keywords: Point kinetics; Multipoint kinetics; APOLLO3; Avery and Kobayashi models; Coupled reactors.

1. Introduction

In this paper, we investigate the main reduced-order approaches to transient analysis in reactor physics. In particular we focus on point kinetics (hereafter PK) [1] and multipoint kinetics (hereafter MPK) [2, 3, 4]. MPK is an advanced zero-dimensional modeling technique that allows to subdivide the reactor in different regions and still consider them as point-like but coupled with each other. In this way we allow for a relative degree of freedom

among them and the neutron population is not forced to evolve rigidly. Several versions of MPK exist [2] but in this paper, we focus on two of them, the one proposed by Avery [3] and the one proposed by Kobayashi [4]. Aside from the theoretical motivation [3, 4] , very few applications of MPK can be found in literature [2, 5] and its interest over PK remains unclear. The purpose of this paper is to stress the differences between those two techniques to better characterize their descriptive capabilities. The novelty of this study is a more precise analysis of behaviors that MPK is able to model but that PK can't reproduce; this is particularly important since some of those behavior can be associated with important changes in the total neutron populations. Thanks to our developments in the neutronic platform APOLLO3 [6] we were able to apply these modeling techniques to two transients. In order to focus on neutronics and on the kinetic response of the systems, the two transients are chosen to be step changes without thermal feedback. In section 2 we briefly describe the various models from the mathematical point of view, trying to focus on their differences; the purpose is to provide an overview of the methods and reference notations. For more complete expositions the reader can consult [1, 3, 4, 5]. To stress the differences between the two modeling approaches we designed a 1D model that, despite being geometrically simple and allowing for a fast calculation of needed quantities, has non-homogeneous properties and permits to test the limit of PK. This model is detailed in section 3. In section 4 we present some results about an early version of the ASTRID reactor [7] that were already obtained in [5] using the code ECCO/ERANOS [8] but that we recompute using the neutronic platform APOLLO3 [6] and a more accurate S_N solver (MINARET [9]). Finally, we present our conclusions and perspectives about these methods based on the experience acquired so far.

2. Mathematical description and notation

The purpose of this section is to fix the notation and give a global overview of the models. Rigorously the neutron flux in a nuclear reactor can be described by the Boltzmann equation:

$$\begin{cases} \frac{1}{v}\frac{\partial \psi}{\partial t} + \mathcal{A}\psi = \mathcal{F}_p\psi + \sum_i \frac{\chi_i}{4\pi}\lambda_i C_i \\ \frac{\chi_i}{4\pi}\frac{dC_i}{dt} = \mathcal{F}_{di}\psi - \frac{\chi_i}{4\pi}\lambda_i C_i \end{cases} , \tag{1}$$

where $\mathcal{F}$ is the fission production operator, $\mathcal{A}$ is the operator containing the transport, removal and scattering term, χ_i is the spectrum and λ_i the

decay constant of the $i-th$ delayed neutron family, ψ is the time dependent neutron flux and C_i is the concentration of precursors of the i-th family. When dealing with the fission operator the convention adopted in this paper is that $\mathcal{F}$ without subscript refers to the total fission operator, with subscript p to the prompt one, with subscript di to the $i-th$ delayed family and with subscript d to the total delayed operator.

This formulation of the Boltzmann equation, however, is used to study nuclear reactors that operate in time dependent condition. In the case of steady state conditions, the second equation in system (1) can be substituted in the first one and we have an homogeneous problem. To allow for a positive non zero solution we have to introduce an eigenvalue or, as is usually done in reactor physics, its reciprocal that is called k-effective (k_{eff}). The resulting equation is:

$$\left(\mathcal{A} - \frac{\mathcal{F}}{k_{eff}}\right)\phi = 0 \qquad . \tag{2}$$

At this point it is worth introduducing also the adjoint formulation of Eq. 2 that is:

$$\left(\mathcal{A}^* - \frac{\mathcal{F}^*}{k_{eff}}\right)\phi^* = 0 \qquad , \tag{3}$$

where the superscript * denotes the adjoint operator or flux. This adjoint flux can be interpreted as the importance of the neutrons relatively to their capability to participate in the chain reaction [10].

A huge effort is devoted to the optimization of the steady state (or critical) calculation and the addition of the time variable leads to very expensive calculations for which significant simplifying assumptions are usually made. The most popular model used in reactor kinetics is PK, that is dealing with the reactor as if it were point-like. In this paper, we are going to analyze how this compares with two others reduced-order models that go under the name of MPK. The MPK approach also consists of dealing with a zero-dimensional model but, instead of using just one point as in the previous method, we split the reactor into different zones and we use a point for each one of them. The consequence of this modeling is that the ordinary differential equation describing the evolution of each region is coupled with the other ones. How to describe this coupling depends on which version of the MPK method we are using.

$$\rho = \frac{\langle \phi^* (\mathcal{F} - \mathcal{A}) \phi \rangle}{\langle \phi^* \mathcal{F} \phi \rangle} \qquad \bar{\Lambda} = \frac{\langle \phi^* \frac{1}{v} \phi \rangle}{\langle \phi^* \mathcal{F} \phi \rangle} \qquad \bar{\beta}_i = \frac{\langle \phi^* \mathcal{F}_{di} \phi \rangle}{\langle \phi^* \mathcal{F} \phi \rangle}$$

$$\bar{\beta} = \sum_i \bar{\beta}_i \qquad \bar{c}_i = \frac{\langle \phi^* \frac{\chi_i^d}{4\pi} C_i \rangle}{\langle \phi^* \frac{1}{v} \phi \rangle}$$

Table 1: Point kinetics parameters

2.1. Point Kinetics

The PK equations were proposed initially by Fermi by means of physical considerations [11] but can be obtained rigorously introducing a factorization of the flux in an amplitude (scalar) and a shape (phase-space distribution), multiplying the time dependent Boltzmann equation by a weight function (usually the adjoint flux), integrating on all variables except time and imposing constraints over the time dependence of the flux shape [1]. The equations that we obtain at the end are the following:

$$\begin{cases} \frac{dT}{dt} = \frac{\rho - \bar{\beta}}{\Lambda} T(t) + \sum_k \lambda_k \bar{c}_k(t) \\ \frac{d\bar{c}_k}{dt} = -\lambda_k \bar{c}_k(t) + \frac{\bar{\beta}_k}{\Lambda} T(t) \end{cases} , \tag{4}$$

where T is the total amplitude of the flux and the other parameters can be found in Table 1.

As we can see, Eq. (4) is a system of ordinary differential equations. From the computational point of view, the solution of these equations is not a critical task and this problem can be tackled with good accuracy and small computation time [5, 12].

The main issue left is the computation of the kinetic parameters that can be obtained as in Table 1. In our convention, $\langle . \rangle$ is the integration over the energy, space, and angular variables and ϕ^* is the static adjoint flux at $t = 0$. Even though any weight function could be used, the standard practice is to use the adjoint flux due to its physical meaning [10] and mathematical properties. No approximation would have been introduced if the forward flux used in the formulas in Table 1 were the time depended flux ψ as it appears in Eq. 1. However, since all the coefficients are obtained through a ratio of fluxes and therefore do not depend on the flux amplitude but just on its shape, the standard way to proceed, in order to avoid to compute the direct time dependent flux, is to use always the direct flux at time 0 and

therefore to neglect any shape change (PK approximation). In conclusion, to implement this method it is enough to compute the critical forward and adjoint fluxes and use them to compute kinetic parameters. Thanks to the solver MINARET [9] we were already able to compute forward and adjoint fluxes but we had to implement a fast method to compute integrals and we had to introduce a delayed nuclear data model to properly define the needed operators [13]. Once all the parameters were obtained the ordinary differential equations were solved thanks to scipy modules [14].

2.2. Multipoint kinetics

2.2.1. Avery's model

The first version of MPK has been proposed by Avery [3] using mainly physical considerations. In this case, we define the partial direct flux and the partial adjoint flux of each region as follows:

$$\mathcal{A}\phi_j = \frac{1}{k_{eff}}\mathcal{F}_j\phi \qquad \mathcal{A}^*\phi_j^* = \frac{1}{k_{eff}}\mathcal{F}_j^*\phi^* \quad , \tag{5}$$

where partial fluxes are defined over the whole reactor and the source term is obtained by restricting the multiplication operator to region j and by using the total flux computed previously (Eq. 2 and Eq. 3). In this case, if we split the reactor in n regions, we have n^2 equations for the evolution of the neutron population and n times the number of precursor families equations for the precursor concentrations. The resulting system is the following

$$\begin{cases} l_{jk}\frac{dS_{jk}}{dt} = k_{jk}(1-\beta_{jk})\sum_m S_{km} - S_{jk} + \sum_i k^d_{jk,i}\lambda_i C_{ki} \\ \frac{dC_{ki}}{dt} = -\lambda_i C_{ki} + \beta_{ki}\sum_m S_{km} \end{cases} , \tag{6}$$

where each parameter can be expressed as in Table 2, again with the approximation that the time-dependent fluxes are replaced with the static ones of Eq. 2 and Eq. 3.

In this model, the partial neutron populations S_{jk} represent neutrons produced in region j by neutrons born in region k and we have an equation for each of them.

2.2.2. Kobayashi's model

Kobayashi's version of MPK has been derived more recently focusing more on a mathematical rigorous approach to the problem [4]. The resulting importances used as weight functions are closer to the Green function definition

$$k_{jk} = \frac{\langle \mathcal{F}_j\phi\rangle\langle\phi^*\mathcal{F}_j\phi_k\rangle}{\langle \mathcal{F}_k\phi\rangle\langle\phi^*\mathcal{F}_j\phi\rangle}k_{eff} \qquad k^d_{jk,i} = \frac{\langle \mathcal{F}_j\phi\rangle\langle\phi^*\mathcal{F}_{dik}\phi\rangle}{\langle \mathcal{F}_{ik}\phi\rangle\langle\phi^*\mathcal{F}_j\phi\rangle}k_{eff}$$

$$l_{jk} = \frac{\langle \phi^*_j \frac{1}{v}\phi_k\rangle}{\langle\phi^*\mathcal{F}_j\phi_k\rangle}k_{eff} \qquad S_{jk} = \frac{\langle \mathcal{F}_j\phi\rangle\langle\phi^*\mathcal{F}_j\phi_k\rangle}{\langle\phi^*\mathcal{F}_j\phi\rangle}$$

$$\beta_{jk} = \frac{\langle\phi^*_j\mathcal{F}_{dk}\phi\rangle}{\langle\phi^*_j\mathcal{F}_k\phi\rangle} \qquad \beta_{ki} = \frac{\langle\mathcal{F}_{dik}\phi\rangle}{\langle\mathcal{F}_k\phi\rangle} \qquad C_{ki} = \langle\frac{\chi^d_i}{4\pi}C_i\rangle_k$$

Table 2: Avery's MPK parameters

$$k_{jk} = \frac{\langle G_j\mathcal{F}_k\phi\rangle}{\langle\mathcal{F}_k\phi\rangle} \qquad k^d_{ijk} = \frac{\langle G_j\mathcal{F}_{dik}\phi\rangle}{\langle\mathcal{F}_{dik}\phi\rangle} \qquad l_j = \frac{\langle G_j\frac{1}{v}\phi\rangle}{\langle\mathcal{F}_j\phi\rangle} \qquad \beta_{jk} = \frac{\langle G_j\mathcal{F}_{dk}\phi\rangle}{\langle G_j\mathcal{F}_k\phi\rangle}$$

$$\beta_{ij} = \frac{\langle\mathcal{F}_{dij}\phi\rangle}{\langle\mathcal{F}_j\phi\rangle} \qquad S_j = \langle\mathcal{F}_j\phi\rangle \qquad C_{ki} = \langle\frac{\chi^d_i}{4\pi}C_i\rangle_k$$

Table 3: Kobayashi's MPK parameters

and are defined as follows:

$$\mathcal{A}^*G_j = \nu\Sigma_{fj} \qquad , \tag{7}$$

where the partial importance here is computed by using as a source the total production cross section restricted to region j, and without using the adjoint flux.

The resulting system of equations is:

$$\begin{cases} l_j\frac{dS_j}{dt} = \sum_k k_{jk}(1-\beta_{jk})S_k - S_j + \sum_i \lambda_i \sum_k k^d_{ijk}C_{ki} \\ \frac{dC_{ki}}{dt} = -\lambda_i C_{ki} + \beta_{ik}S_k \end{cases} , \tag{8}$$

where the unknown neutron populations S_j are the populations of each region independently from where the neutrons which generate them were coming. Therefore the resulting system has fewer equations for the population evolution (as many as the number of regions) but the same amount for the precursors concentrations. Parameters can be computed as in Table 3.

2.3. Comments

The main differences among the methods described so far result from the weight functions selected. PK uses the adjoint flux that is a measure of the importance of neutrons relative to their capability to participate in

the chain reaction [10]. Avery's MPK uses a partial version of forward and adjoint fluxes (Eq. (5)) that add to total the respective fluxes used in PK. Kobayashi's importances instead can be seen as the capability of the neutron to reproduce neutrons, but at the next generation only, not over the total chain reaction [5]. The calculation of these importance functions has been implemented in APOLLO3.

We would like also to add that all the methods described so far can be expressed in the compact form:

$$\frac{dS}{dt} = \mathcal{M}S \qquad , \tag{9}$$

where the size of vector S and of matrix $\mathcal{M}$ depends on the method we are using, in particular, if S is vector of length n, $\mathcal{M}$ is a $n \times n$ square matrix. In our case, since we are using the JEFF 3.1.1 nuclear data library, we use 8 precursor families [15]. Therefore for PK the S vector has 9 elements (8 for the precursor families and one for the neutron population). For Kobayashi's MPK, if the number of regions in which we are subdividing our reactor is n, the S vector has $9n$ elements, n for the neutron populations, and $8n$ for the precursors in each region. For Avery's MPK, S has $(8+n)n$ elements, n^2 for the neutron populations, and $8n$ for the precursors in each region. The study of the eigenvalues of $\mathcal{M}$ can provide useful information about the transient, as it is discussed in the next sections. Finally we would like to define the prompt sub-matrix as the square matrix that we obtain from the total one ($\mathcal{M}$) by eliminating lines and columns concerning precursors. This matrix will be the one associated to a model in which precursors do not exist. To clarify this definition we make the example for the associated model in the Kobayashi's case:

$$l_j \frac{dS_j}{dt} = \sum_k k_{jk}(1-\beta_{jk})S_k - S_j \qquad . \tag{10}$$

The comparison between the eigenvalues of the prompt sub-matrix and of the total one can help us to identify the source of the different behaviors.

3. 1D Model

The first system we choose to model is a simplified 1D model of a coupled thermal-fast reactor. Although being an extremely simplified configuration,

this model aims at having short computation time while retaining some heterogeneity that can highlight the differences among the modeling techniques presented so far. The description of this system can be found in [16] and a synthetic description of the materials and its properties can be found in [17]. Originally it was described by an RZ geometry but we preferred to adopt a 1D geometry since it is simpler and can be handled by our solver (MINARET [9]). The core is divided into 6 regions as can be seen in Fig. 1 where reflection condition is applied to the left boundary and vacuum condition to the right one; from left to right there is a central fast zone (Fast, F), a filter to absorb thermal neutron (Absorber, A), a natural uranium transition zone (Buffer, B), an enriched uranium plate (Converter, C), a thermal zone (Thermal, T) and a water reflector (Water, W).

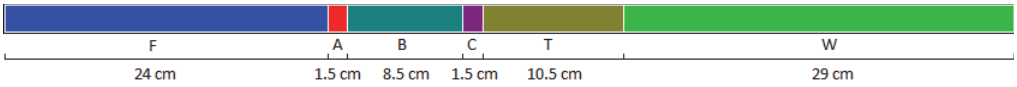

Figure 1: 1D model of a coupled fast-termal reactor

The material used for the fast zone is the cell used in the ERMINE V program of the MINERVE experimental reactor, in the center of the ZONA-1 core [18]. This cell is composed of 6 MOx rodlets, 2 natural UOx rodlets, and 8 sodium rodlets, combined in a 2 inch square. The filter to absorb thermal neutron is made up of natural B_4C rodlets and the natural uranium in the transition zone is in the form of UO_2 rodlets. The UO_2 rodlets in region C are enriched at 30% in ^{235}U and the the UO_2 in the thermal zone has 3.7% enrichment. Water is present only in the thermal zone and in the reflector. All the materials have been homogenized by ECCO/ERANOS [8] and provided to APOLLO3® using a 33 groups energy mesh (more detail can be found in [16, 17]).

The basic idea behind this configuration is that the absorber, the buffer and the converter help to decouple the fast zone from the thermal one, being these the two zones where most of the fissions take place.

We can then introduce a perturbation, removing the absorber and the converter. In this way, we change the kinetic parameters of the reactor keeping the reactivity insertion positive but below prompt criticality (β=586pcm and ρ=284pcm). In order to do so we artificially replace the material in the converter zone (enriched uranium) with the one in the buffer zone (natural uranium) and remove 92% of the ^{10}B in the absorber zone.

PK (k_{eff})	1.11706
Kobayashi (k_{ij})	$\begin{bmatrix} 0.88923 & 0.29334 & 0.15291 & 0.05134 \\ 0.03203 & 0.12125 & 0.07372 & 0.02288 \\ 0.12134 & 0.28680 & 0.38487 & 0.19834 \\ 0.16048 & 0.41637 & 0.56683 & 0.77045 \end{bmatrix}$
Avery (k_{ij})	$\begin{bmatrix} 0.89357 & 0.28779 & 0.15006 & 0.05032 \\ 0.03211 & 0.12127 & 0.07364 & 0.02286 \\ 0.12139 & 0.28695 & 0.38502 & 0.19824 \\ 0.16864 & 0.43211 & 0.58580 & 0.75710 \end{bmatrix}$

Table 4: k_{eff} and k_{ij} of the nominal configuration (before division by k_{eff})

In order to keep the transient simple and to focus on the neutronics, we simulate an instantaneous change without considering thermal feedback. The system is supposed to be at t=0 in steady state in the nominal configuration and to shift instantaneously to the perturbed configuration. In order to have a steady state system at t=0, we divide all the coupling matrices and generation times by the k-effective of the nominal configuration, that is 1.11706.

3.1. Results

In this section, we present five sets of results. One set is obtained by applying PK, and four are obtained by applying MPK. For MPK we have 2 sets using four regions, one for each homogeneous fissile zone, that are F, B, C and T in Fig. 1, both with Kobayashi's and with Avery's models, and two sets using 6 regions, where we split in half the 2 main fissile regions that are F and T.

As an example, we present the main kinetic parameters and coupling matrices we obtained for the nominal case. The k_{eff} and k_{ij} are listed in Table 4, mean generation time and relative MPK versions in Table 5 and beta effective and β_{ij} in Table 6. A first observation can immediately be made on the data presented in Table 4, the first of the four eigenvalues of

PK (Λ) [μs]	9.9915
Kobayashi (l_j) [μs]	$\begin{bmatrix} 0.3125 \\ 0.4241 \\ 3.7227 \\ 28.232 \end{bmatrix}$
Avery (l_{ij}) [μs]	$\begin{bmatrix} 0.2465 & 0.3491 & 0.3935 & 0.4495 \\ 0.2938 & 0.1370 & 0.2646 & 0.6829 \\ 2.8120 & 2.5776 & 2.4007 & 4.2755 \\ 17.8861 & 18.8878 & 19.1796 & 25.4637 \end{bmatrix}$

Table 5: Λ, l_j and l_{ij} of the nominal configuration (before division by k_{eff})

PK (β_{eff}) [pcm]	586.9
Kobayashi (β_{ij}) [pcm]	$\begin{bmatrix} 332.4 & 1097.1 & 497.3 & 299.2 \\ 119.3 & 289.9 & 170.0 & 194.4 \\ 339.8 & 1486.3 & 776.3 & 715.0 \\ 304.2 & 1371.8 & 727.6 & 807.3 \end{bmatrix}$
Avery (β_{ij}) [pcm]	$\begin{bmatrix} 332.7 & 1097.1 & 496.7 & 298.4 \\ 119.2 & 289.9 & 170.0 & 194.3 \\ 339.8 & 1486.1 & 776.2 & 714.7 \\ 307.7 & 1390.7 & 738.7 & 809.4 \end{bmatrix}$

Table 6: β_{eff} and β_{ij} of the nominal configuration

both k_{ij} matrices is equal to k_{eff}, as it should be by construction. This is a first verification of our implementation and shows how, in MPK, k_{ij} has a role similar to the one that k_{eff} has in PK. Regarding the data in Table 5 they represent the mean neutron generation life time. These data are mainly sensitive to the neutron spectrum and show how the spectrum gets softer moving towards the thermal zone (last line). We can also observe that, looking at the Avery's l_{ij}, discriminating the various regions where neutrons are generated (different columns represent different departing regions) has limited effects with respect to the importance that has the region where the neutrons end (different lines represent different ending regions). Finally looking at data in Table 6 we can see how the delayed neutron fraction has a very heterogeneous distribution, mainly depending on where neutrons are produced (therefore presenting similar values along each column). We can also notice, in the second line, how the neutrons ending in the natural uranium zone (zone B in Fig. 1) have considerably smaller effective delayed fraction with respect to the neutrons born from the same region but ending in a different one. This can be explained thanks to the ^{238}U fission threshold that prevents most of the delayed neutrons from any region (that have a softer spectrum compared to the prompt ones) to participate in the chain reaction by inducing fission in the buffer region containing mainly ^{238}U as fissile nuclide.

The first quantity on which we would like to focus on is the total neutron population evolution during the transient that can be seen in Fig. 2.

On a short time scale, as we can notice, there is a huge difference between the results obtained with PK and those obtained with MPK, while all the MPK cases provide similar results. In particular, all the MPK curves have a bump before $10^{-5}s$ that is completely absent in the PK one. After that, there is the classical prompt jump that, however, in the MPK cases has a bigger amplitude. Looking at the differences among the various MPK, subdividing the main regions has virtually no effect on the Avery modeling and leads to a slight increase of the total neutron population modeled by Kobayashi MPK. Compared to Avery, Kobayashi has a slightly bigger population before the prompt jump and slightly smaller afterwards, although all these are minor differences and can be due to the various approximations made during the modeling.

Looking at Fig. 3 we can see the relative distribution of the neutron population in the various regions. We can notice how the redistribution of the neutron population takes place at the same time as the first bump in the

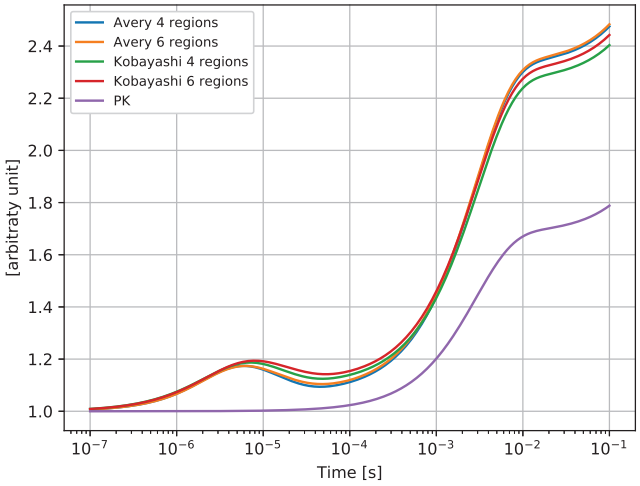

Figure 2: Total neutron population evolution - 1D model

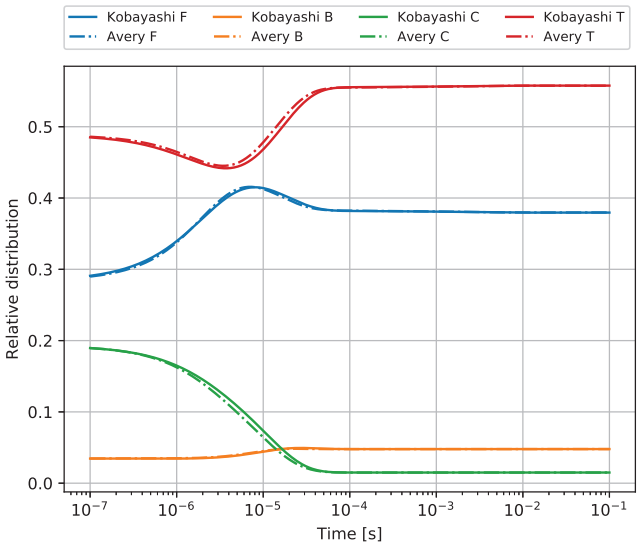

Figure 3: Relative neutron population evolution - 1D model

total population evolution and is almost complete before the prompt jump. We can also notice that no major difference appears between Kobayashi's and Avery's models.

Concerning the long time scale (Fig. 4), all models present a coherent

exponential behavior with Kobayashi's model having a slightly different time constant with respect to the other results and that changes slightly with the further subdivision of the main fissile zones. This effect, even though of

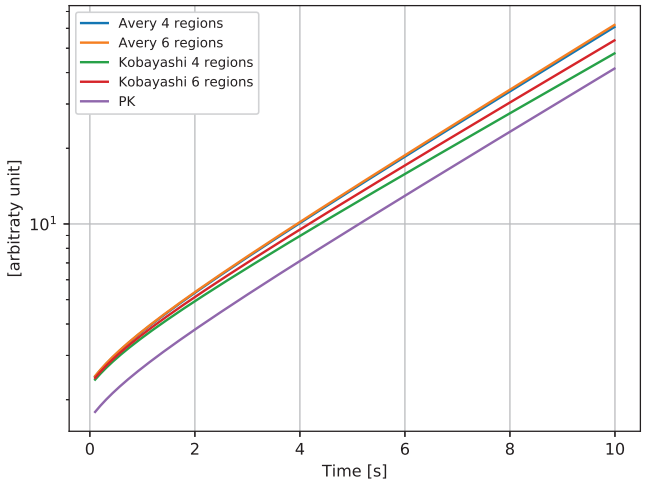

Figure 4: Asymptotic neutron population behavior - 1D model

second order, could be due to the approximations made (e.g. the use of the k-modes instead of the alpha-modes) and should be further investigated.

To conclude we can look at the eigenvalues of the matrix $\mathcal{M}$ (Eq. 9) in the different models, plotted in Fig. 5 where on the horizontal axis we have the real part of the eigenvalues on a symmetric log scale. We have to remark that all the eigenvalues are real, except for Avery's MPK with 6 regions that has a few complex eigenvalues; in all the cases however the real part is much larger than the imaginary part meaning that the damping effect is dominant with respect to the oscillating behavior and therefore we focus only on real parts.

In the first line we plotted the decay constant of each precursor family, so to show how some of the various eigenvalues cluster around the eight $(-\lambda_i)$ with a multiplicity equal to the region number (as already discussed by Henry [19]). As expected, in all the cases, we have one positive eigenvalue with similar value for all the methods (with the biggest discrepancy being between Avery's and Kobayashi's models of about 7%) Then, for MPK, we have the appearance of several eigenvalues all on a very short timescale. For

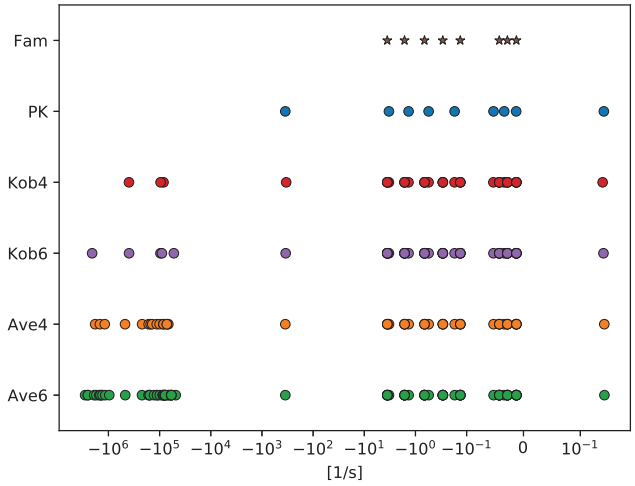

Figure 5: Eigenvalues of the 1D model

all the MPK models, if we compare these eigenvalues (those $< -10^2\ s^{-1}$) with the ones of the relative prompt sub-matrix, we notice that we obtain the same eigenvalues (maximum relative error below 10^{-8}), except for the one relative to the prompt jump (around $-5 \cdot 10^2\ s^{-1}$) for which we have, in all the models, a relative error of 0.3%. This shows how the bump noticed in Fig. (2) is mainly due to the prompt behavior of the system.

4. ASTRID

The second system we modeled is an early sodium-cooled fast reactor ASTRID CFV core design [7] shown in Fig. 6. The core has a $2\pi/3$ rotational symmetry and for the application of the MPK we chose symmetric regions as shown in Fig. 6. The transient we analyzed is a step change where the red-circled rod in region 1 is instantaneously removed from the core. The same transient has been analyzed in [5] with the ECCO/ERANOS code [8].

Also here we are below prompt criticality (β=369pcm and ρ=349pcm) but with much smaller margin.

4.1. Results

In this case, we present three sets of results, one for the PK and two for the MPK, one for Avery's model and one for Kobayashi's model. The

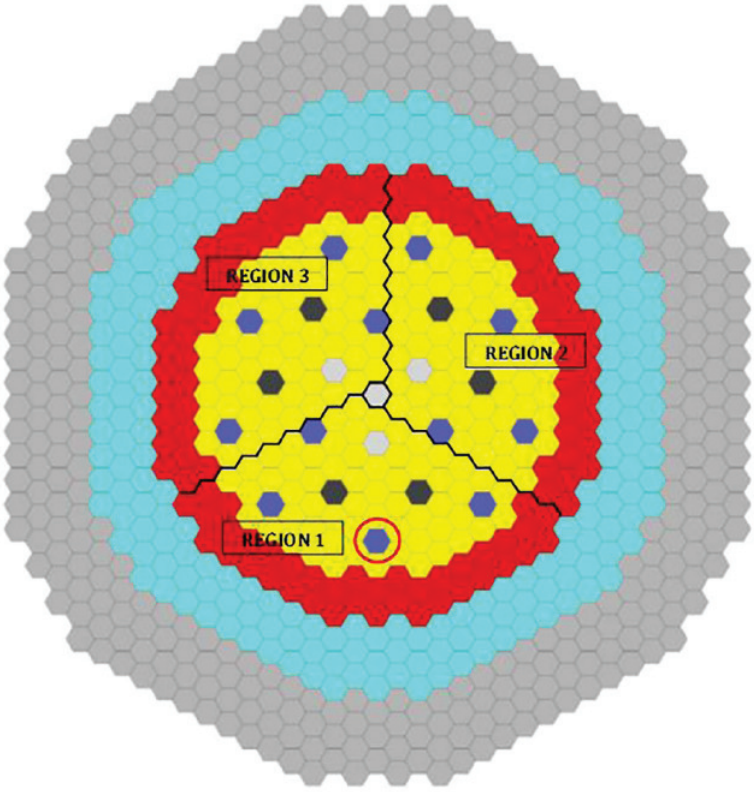

Figure 6: ASTRID CFV-V1 - Color code: Yellow: inner fuel - Red: outer fuel - Light blue: reflector - Grey: shielding - Dark blue and black: control rods - White: inert sub-assemblies

total population evolution is plotted in Fig. 7. Here, as opposed to what happens in the previous case, there is no major difference between the various modeling techniques for what concerns the total population.

However, if we look at the population repartition in Fig. 8 we can see in the MPK models quick changes in the neutron population distribution taking place in the same timescale as the previous case and before the prompt jump. The main difference is that, in this case, the redistribution of the neutron population is not associated with a change in the total amplitude.

For what concerns the asymptotic behavior (Fig. 9) no major differences exist among the various models, with existing discrepancies that, also in this case, we think can be explained by the different approximations we did.

Looking at the eigenvalues of the matrix $\mathcal{M}$ (Eq. 9) in Fig. 10 we can see how, also in this case, some eigenvalues cluster around the opposites of

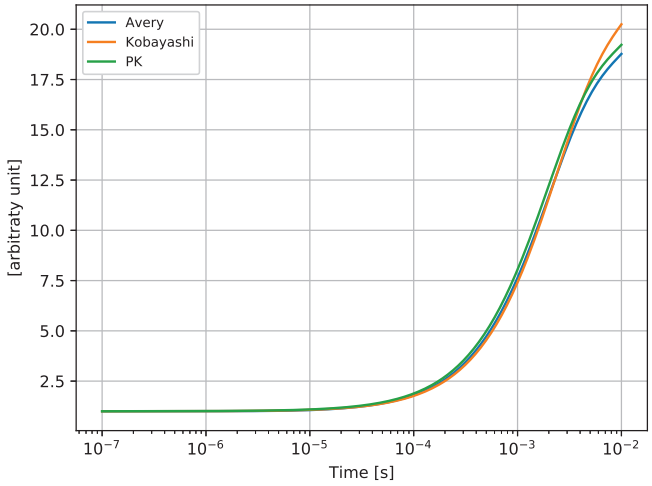

Figure 7: Total neutron population evolution - ASTRID model

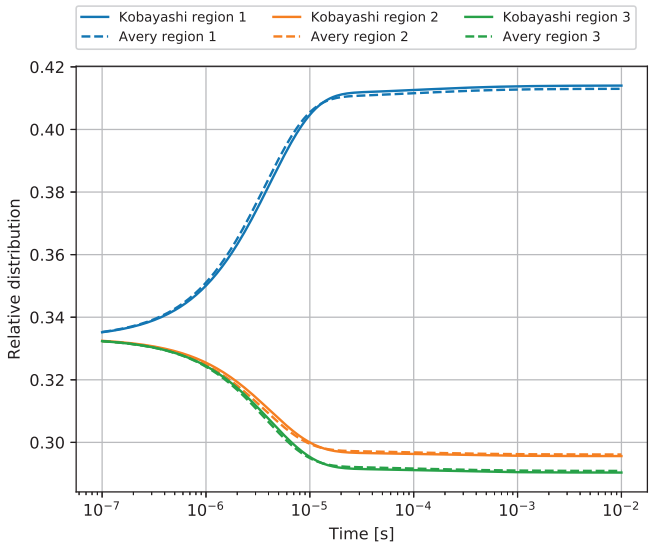

Figure 8: Relative neutron population evolution - ASTRID model

the decay constants of precursor families. We notice also the single positive eigenvalue with similar value for all the models (with the biggest discrepancy being between PK and Kobayashi's MPK of about 8%) and that MPK presents a set of smaller eigenvalues enabling shape changes on a very short

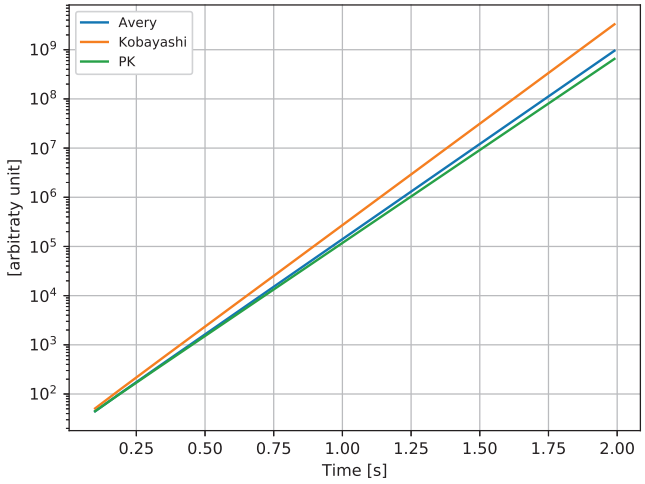

Figure 9: Asymptotic neutron population behavior - ASTRID model

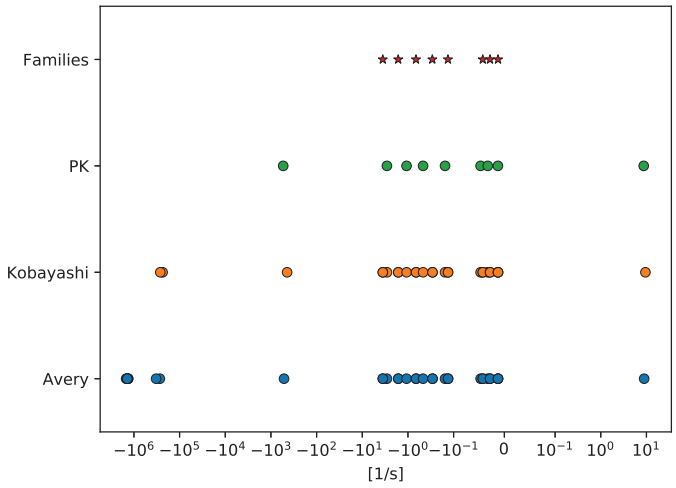

Figure 10: Eigenvalues of the ASTRID model

timescale. Also here, for all the MPK models, if we compare these eigenvalues (those $< -10^2\ s^{-1}$) with the ones from the one of the prompt sub-matrix we notice that we get the same eigenvalues (maximum relative error below 10^{-8}), except for the eigenvalue around $-5 \cdot 10^2\ s^{-1}$ for which we have a rel-

ative error of 2%. This seems to show that, as the reactor approach prompt criticality, the leading prompt eigenvalue is more influenced by the total system and we have higher deviation from the one of the prompt sub-matrix alone.

5. Conclusions and perspectives

The discussion of the results presented shows that in the cases considered, there are minor differences between Avery's and Kobayashi's formalisms. We also show how a further subdivision of homogeneous zones, in the cases considered, has a small impact on the overall description of the system. However, in the heterogeneous case, MPK is able to model total flux changes that PK is not able to reproduce and therefore MPK constitutes an important improvement in transient modeling. These results seem to show that, concerning the region subdivision in MPK, it is important to separate regions with different kinetic proprieties but further subdivision of homogeneous regions has a minor impact.

We also noticed that, after a step perturbation, the repartition of the neutron distribution anticipates the prompt jump and the following exponential behavior of the total amplitude.

While in this work we focused on the characterization of PK and MPK, limiting our analysis on the capabilities of the two methods, further work should be done to validate the results presented so far; this can be done by comparison against direct kinetic calculation, either deterministic or Monte Carlo, or against experimental data.

As perspectives, we think it is interesting to further investigate the evolution of the eigenvalues with respect of different criticality situations, including more accurate analyses around prompt criticality. We also think it is interesting to reproduce these results using fluxes different from the ones obtained using the k-modes from Eq. (2) and (3) [e.g. alpha modes (temporal eigenvectors) or even dynamic fluxes if MPK is included in a quasi-static space-time kinetic scheme] that could be more representative of the analyzed cases. Finally we would like to combine these results with the work done in [20] to predict the flux shape evolution and to optimize shape calculation time step during transients.

[1] A. Henry, The application of reactor kinetics to the analysis of experiments, Nuclear Science and Engineering 3 (1) (1958) 52–70.

[2] S. Dulla, P. Picca, Consistent multipoint kinetics for source-driven systems, Progress in Nuclear Energy 48 (7) (2006) 617–628.

[3] R. Avery, Theory of coupled reactors, Proc. 2nd UN Int. Conf. Peaceful Uses of Atomic Energy, United Nations 12 (1958) 182.

[4] K. Kobayashi, Rigorous derivation of multi-point reactor kinetics equations with explicit dependence on perturbation, Journal of Nuclear Science and Technology 29 (2) (1992) 110–120.

[5] J. Tommasi, G. Palmiotti, Verification of iterative matrix solutions for multipoint kinetics equations, Annals of Nuclear Energy 124 (2019) 357–371.

[6] D. Schneider, F. Dolci, F. Gabriel, J.-M. Palau, M. Guillo, B. Pothet, APOLLO3: CEA/DEN deterministic multi-purpose code for reactor physics analysis, in: Proc. Int. Conf. PHYSOR 2016, American Nuclear Society, Sun Valley, Idaho, United States, 2016.

[7] F. Varaine, P. Marsault, M.-S. Chenaud, B. Bernardin, A. Conti, P. Sciora, C. Venard, B. Fontaine, N. Devictor, L. Martin, A.-C. Scholer, D. Verrier, Pre-conceptual design study of ASTRID core, 2012.

[8] J.-M. Ruggieri, J. Tommasi, J.-F. Lebrat, S. Christophe, D. Plisson-Rieunier, C. De Saint Jean, G. Rimpault, J.-C. Sublet, ERANOS 2.1 : International code system for GEN IV fast reactor analysis, 2006.

[9] J. Moller, J.-J. Lautard, D. Schneider, MINARET, a deterministic neutron transport solver for nuclear core calculations, in: Proc. Int. Conf. on Mathematics and Computational Methods Applied to Nuclear Science and Engineering (M&C2011), American Nuclear Society, 2011.

[10] L. Usachev, Equation for the importance of neutrons, reactor kinetics and the theory of perturbations, in: Proc. Int. Conf. on the Peaceful Uses of Atomic Energy, Geneva, Switzerland, Aug. 8-12, 1955, Vol. 5, 1956, pp. 503–510.

[11] E. Fermi, Problem of time dependence of the reaction rate: effect of delayed neutrons emission, Tech. rep., Report CP-291 (Notes on Lecture of October 1942).

[12] B. Ganapol, A refined way of solving reactor point kinetics equations for imposed reactivity insertions, Nuclear Technology and Radiation Protection 24. doi:10.2298/NTRP0903157G.

[13] G. Valocchi, P. Archier, J. Tommasi, Beta effective sensitivity to nuclear data within the APOLLO3 neutronic platform, in: Proc. Int. Conf. PHYSOR 2020, American Nuclear Society, Cambridge, England, 2020.

[14] P. Virtanen, et al., Scipy 1.0-fundamental algorithms for scientific computing in python, CoRR abs/1907.10121. arXiv:1907.10121.
URL http://arxiv.org/abs/1907.10121

[15] G. Rudstem, P. Finck, A. Filip, A. D'Angelo, R. McKnight, Delayed neutron data for the major actinides. vol. 6, Nuclear Energy Agency Report NEA/WPEC-6.

[16] P. Ros, Conception neutronique de configurations experimentales a forte adaptation spectrale en reacteur de puissance nulle pour des applications multi-filieres Gen-II,III & IV, Ph.D. thesis, 2017GREAI045 (2017).
URL http://www.theses.fr/2017GREAI045

[17] P. Ros, P. Leconte, P. Blaise, J. Di-Salvo, Fast-thermal coupled cores in ZPR revisited: physical specificities and potentialities for ZEPHYR, in: PHYSOR Conference, Sun Valley, 2016.

[18] L. Martin-Deidier, Mesure intégrale de la capture des produits de fission dans les réacteurs à neutrons rapides, Ph.D. thesis (1979).

[19] A. F. Henry, The application of inhour modes to the description of non-separable reactor transients, Nuclear Science and Engineering 20 (3) (1964) 338–351. arXiv:https://doi.org/10.13182/NSE64-A19579, doi:10.13182/NSE64-A19579.
URL https://doi.org/10.13182/NSE64-A19579

[20] D. Caron, S. Dulla, P. Ravetto, Adaptive time step selection in the quasi-static methods of nuclear reactor dynamics, Annals of Nuclear Energy 105 (2017) 266–281.